# Quarterly Report

**Date of report:** April 13, 2007

**For quarter ending**: March 31, 2007

**Agreement number:** DTPH56-06-X-000029

**Agreement Time period**: June 30, 2006 to June 29, 2008

**Project:** Mechanical Properties and Crack Behavior in Line Pipe Steels

**Prepared by:** NIST, Materials Reliability Division

**Project Tasks:**
**Task 1:** Fatigue crack growth
**Task 2:** Hydrogen charged fatigue crack growth
**Task 3:** CTOA testing and modeling
**Task 4:** Fracture surface examination
**Task 5:** Method for determination of yield strength in high strength pipeline steels and welds
**Task 6:** Other tasks as assigned
**Task 7:** Reporting

NIST-Boulder received the contract for this program in early June 2006. Since this contract started, our efforts have been focused on CTOA testing of weldments and their heat affected zones (girth and seam) and on the development of the model for our dynamic ductile fracture experiments. We have completed the design and construction of the dynamic CTOA apparatus and the system was tested late this reporting period. Full-thickness fatigue experiments and hydrogen charged specimen testing is underway.
The following task updates should be appended to previously submitted quarterly reports.

## Technical status of tasks:

### Fatigue crack growth

The axial fatigue tests continue at r=0.1 and 0.4. The axial specimen testing is almost complete and we plan to finish this portion of the effort within the next quarter. At that time we plan to start the transverse specimen fatigue testing, with the fatigue crack propagating along the pipe axis. The uneven fatigue crack propagation through the pipe wall thickness in a couple of the specimens has prompted us to investigate this phenomenon further. We have ordered software that will allow us to monitor and record the fatigue crack growth on both the ID and the OD of the pipe wall, enabling us to better understand this uneven crack growth.

**Hydrogen charged fatigue crack growth**

Specimen charging is still underway for this effort. We expect to have two specimens available for testing within the next 3 weeks, along with results of the diffusion rate studies being conducted as the specimens are charging. The results of this task are expected to be completed within the next quarter. Following the completion of the testing portion of this task, we plan to conduct examinations of the fracture surfaces to determine the fracture morphology in the charged and uncharged areas.

**CTOA testing and modeling**

CTOA specimen testing is underway on both girth and seam weld direction fracture specimens. Previous efforts were focused on base metals with cracks oriented in the axial direction. The current effort continues to examine fracture resistance along the girth weld and girth heat affected zone (HAZ) as well as base metal in the girth direction. In addition, seam weld CTOA specimens are being machined to study ductile fracture resistance in the HAZ of the seam weld and weld metal, and specimens are being machined and tested with the crack propagating across the girth weld. Data from one of these tests is shown in Figure 1. This data clearly shows the effects of the HAZ and weld on the CTOA.

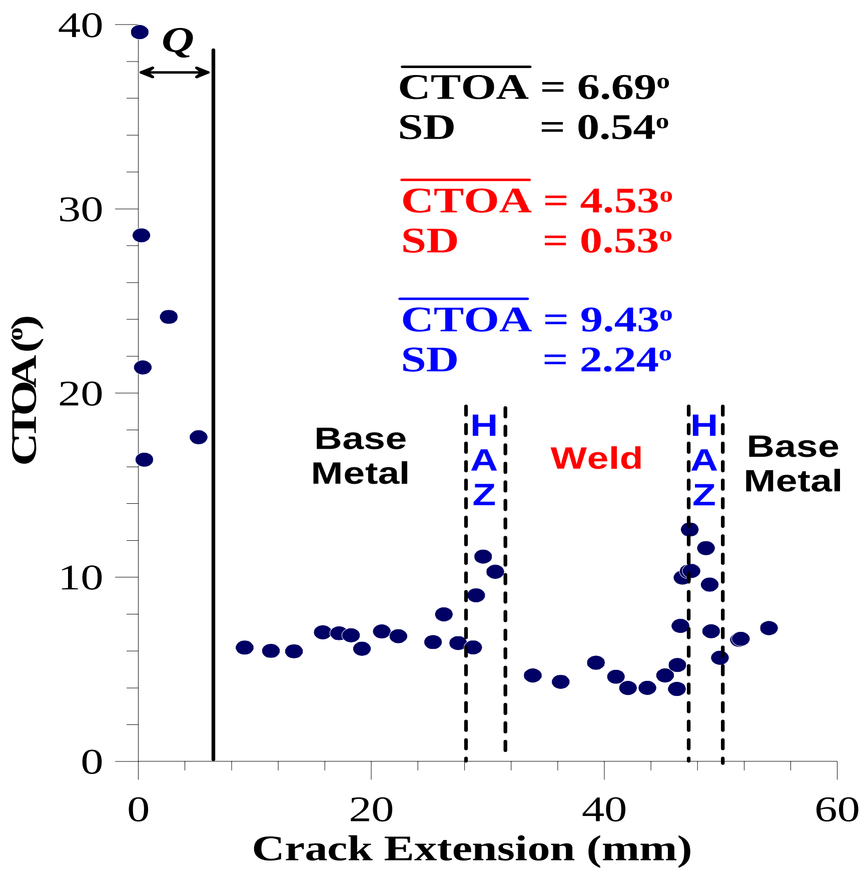


**Figure 1.** CTOA vs crack extension showing an increase in ductile fracture resistance in the HAZ and a decrease in the harder weld area, as compared to the base metal.

**Dynamic CTOA Testing**

In order to conduct high rate (dynamic) CTOA tests, we upgraded our high-rate 500 kN servo-hydraulic machine with a new controller and designed and machined grips (Figure 2) and associated fixtures that allowed us to test to the machine's rate limits. The high rate capacity is on this particular machine is not dynamic as compared to the Kolsky tester (strain rates of $10^3\,s^{-1}$ to $10^4 s^{-1}$) but is dynamic as compared to the standard quasi-static cross-head rates ($10^{-3}$ mm/s) on the typical CTOA tests. The cross-head rates we expect to be able to test on this machine are on the order of 250 mm/s, an increase of 5 orders of magnitude over the lowest quasi-static rates tested in our laboratory. The crack velocity appears to be approximately double the crosshead rate with our fixture design. The crack velocity is dependent on the crosshead velocity, the specimen ductility and the specimen geometry.

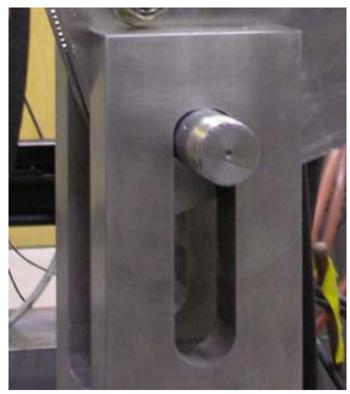

(a) (b)

**Figure 2:** The dynamic CTOA clevis configuration, (a) Upper clevis, (b) Lower clevis with the slot.

Because we expect an increase in load with an increase in strain rate, we designed the clevis grips and load plates for a higher load capacity than those used for the quasi-static tests. The lower clevis was designed with a slot in order to allow the upper clevis (with specimen attached) to reach a constant speed before the lower clevis engaged, loading the specimen at the desired rate.

In order to monitor and record the CTOA during the test, we use a high speed camera, a personal computer with special software and a crack-mouth opening gage. The test system appears in Figure 3.

We are currently modifying the image data acquisition system in hopes of streamlining the CTOA measurements, but only if the data quality is as good as currently used methods. One of the drawbacks to CTOA measurement is the inconsistency in the determination of the angle. As part of our research effort, we are evaluating both direct (optical microscopy and digital image correlation) and indirect (micro-topography and force-displacement diagram) measurement methods, both of which are included in the ASTM and ISO draft standards for CTOA testing.


**Figure 3**: The dynamic CTOA test system.

We machined aluminum dummy specimens to test the machine and load-train performance. The specimen failed in the bolts, but the system design performed as expected, paving the way for the first pipeline steel dynamic CTOA test.
The initial dynamic test on a steel specimen was conducted on X65 pipeline steel (Figure 4). The test performed very well and the data is under analysis now and will be reported in the next quarterly report.

**Figure 4:** X65 steel specimen after the test.

For the next quarter, we plan to conduct dynamic rate tests at two rates, on two different steels, but in only one thickness, 8 mm. Test results from these specimens will be compared to results from the slower quasi-static tests. The test system, as well as the specimen grip system will be evaluated for performance as the testing progresses.

**Dynamic Kolsky Bar Testing**

The high strain rate plastic flow properties of high strength pipeline steels at sub-ambient temperatures will be examined at NIST Gaithersburg using a temperature controlled Split-Hopkinson Pressure Bar (Kolsky Bar) apparatus. For a running ductile fracture in a gas pipeline, the ability of a steel to strengthen near the crack tip, where the strain rate is very high, has an important impact on the propagation and arrest behavior of the fracture. Strain rate effects on the strengthening of different grades of pipeline steel have already been investigated at ambient temperature using the Kolsky Bar. We will now extend the study to examine how temperature influences the strengthening behavior of these steels with increasing strain rate. Decreasing temperatures tend to increase the strength of steel, much like increasing strain rates. As a result, the capacity of steel to strengthen may decrease with temperature, meaning ductile fractures may propagate more easily in pipelines that are buried in cold environments. Kolsky Bar measurements of pipeline steels will be used to help discriminate the strain rate strengthening capacity of available pipeline steel materials at cold temperatures, so that optimal fracture-resistant steels can be chosen for high pressure gas pipelines.

**CTOA Fracture Surface Evaluation:**

In addition to the weld specimens mentioned above, we also focused on quasi-static CTOA testing of X65 and X100 steels, using both 3 and 8 mm thick Modified Double Cantilever Beam specimens. The fracture surfaces from these tests indicate that the 8 mm thickness is needed to promote the desired slant fracture mode for the steels and loading rates evaluated. In Figure 5, for example, the X100 3 mm specimens typically show a combination of slant and flat type fractures, with extensive thinning (necking) associated with flat fracture regions. For the 8 mm specimen thickness, however, the X100 has extended regions of slant fracture, as shown in Figure 2.

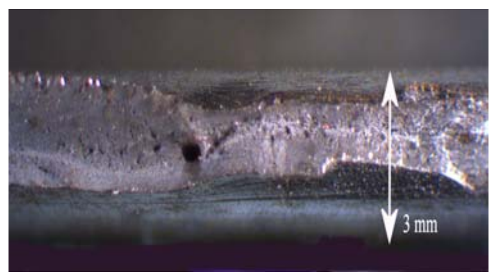


**Figure 5:** X100 3 mm CTOA specimen showing combined slant (on left) and flat fracture mode.

The fracture surface in Figure 6 is associated with the initial portion of an 8 mm CTOA test, and it shows 3 characteristic features for X100 steel specimens we tested: (1) as might be expected, there is a significant decrease in the plastic flow (thinning from the original thickness to a lesser thickness) associated with the slant fracture mode, (2) the curvature of the crack front results in a

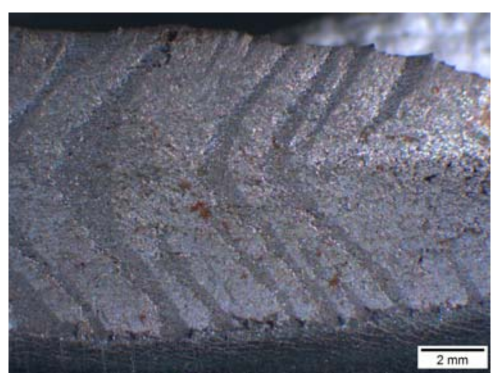


**Figure 6:** X100 8 mm thick CTOA showing region of transition from flat (right) to slant (left) fracture.

difference of about 2 mm between crack front at the outside surface and center of the 8 mm thick specimen, (3) the slant fracture surface is almost flat and at about 45 degrees to the load line of the specimen. These characteristics will be compared with those of fractures of this same X100 material from full scale burst tests, and other laboratory tests conducted at a variety of loading rates.

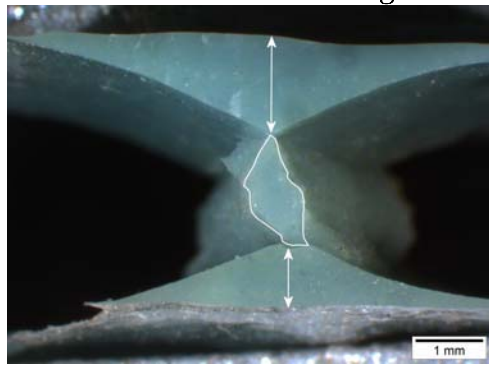


**Figure 7:** Casting of fracture void in an X65 8 mm thick CTOA specimen, showing extent of thinning (arrows) and cross sectional shape of void behind the crack tip.

This quarter we also evaluated several techniques to produce a cast of the void shape just behind the crack front. Figure 7 shows a silicone rubber cast of the fracture void (tunneling) ahead of the crack tip in an 8 mm thick X65 CTOA specimen. This work is in support of 2-D to 3-D modeling efforts. We plan to use the technique to provide a reasonable quantitative description of the crack front shape and position through the thickness of the specimens.

Enlarged photos of the fracture surface figures are shown below.

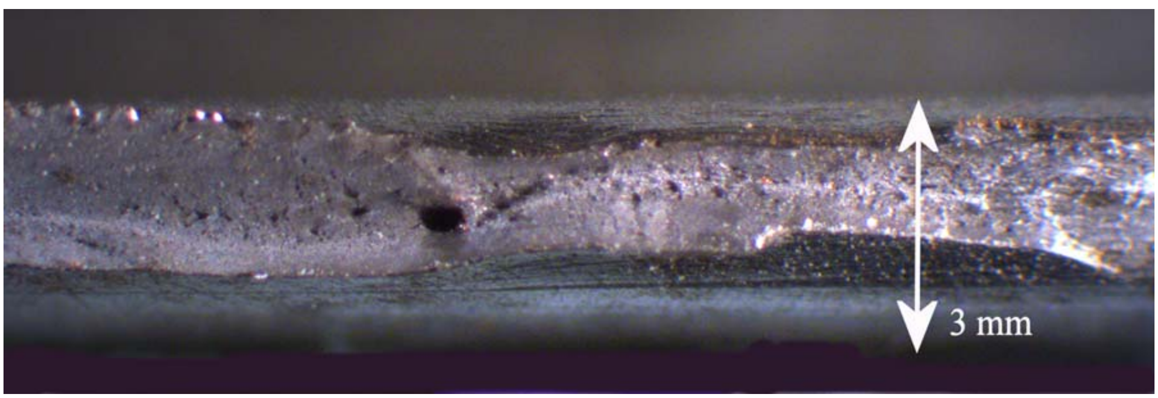


The fracture surface of a 3 mm thick CTOA specimen of X100 steel is shown. The fracture consists of a mixture of slant and flat fracture morphologies, and there is extensive thinning through the thickness of the specimen, particularly within the flat fracture regions. The arrows approximate the original thickness of the specimen.

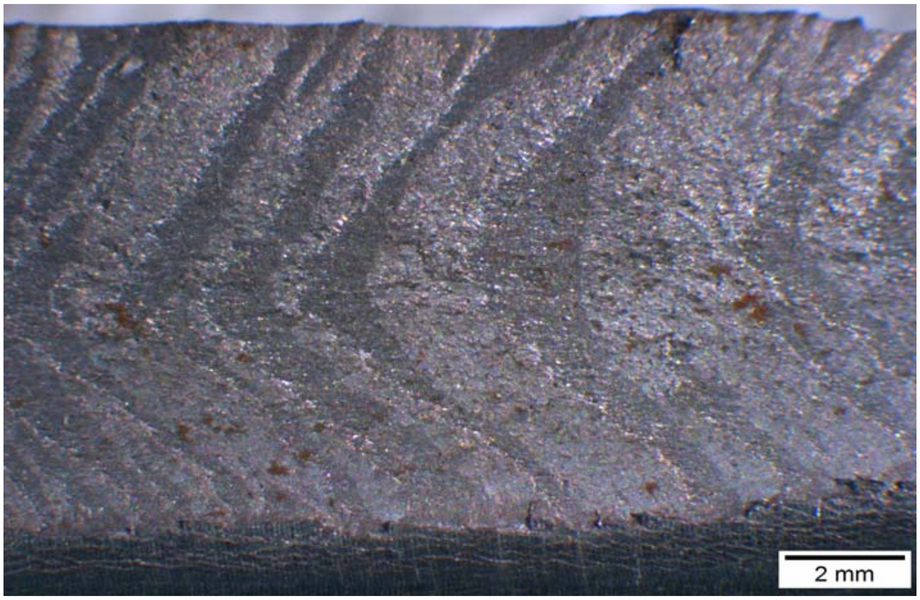


The markings on the fracture surface of the X100 CTOA specimens (8 mm thick) show the shape of the crack front as it grew down the specimen during the test. Typically, the curvature of the crack front on these specimens results in a difference between the crack tip and the surface of about 2 mm.

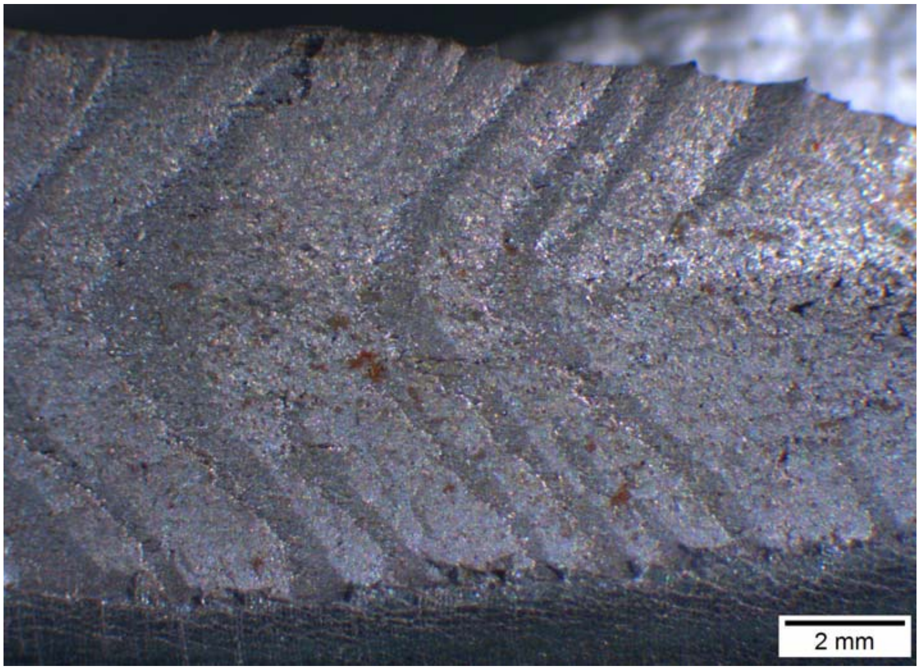


The fracture surface of an 8 mm thick CTOA specimen of X100 steel is shown. The region shown includes the transition from flat (right) to slant (left) fracture that occurs during the initial portion of the CTOA test. The thinning of the specimen thickness decreases significantly in slant fracture regions.

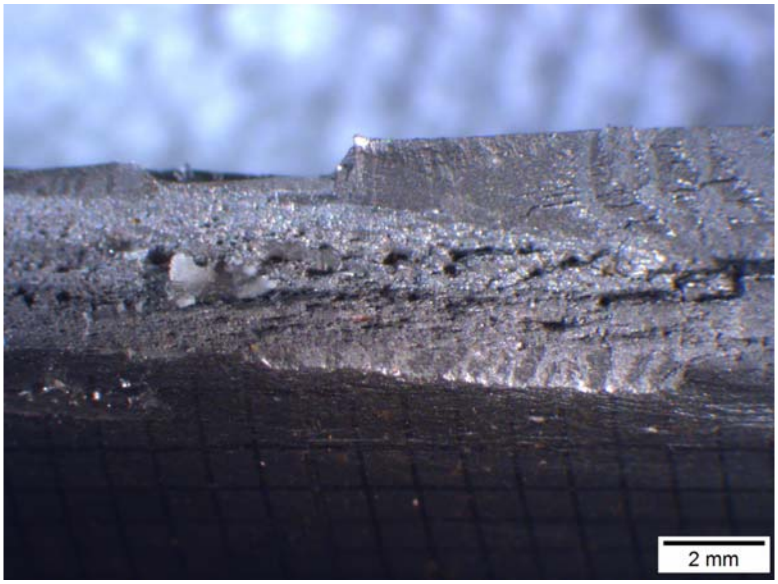


The fracture surface of this 8 mm thick X65 CTOA specimen shows a mixture of slant and flat fracture. This is typical of our results to date.

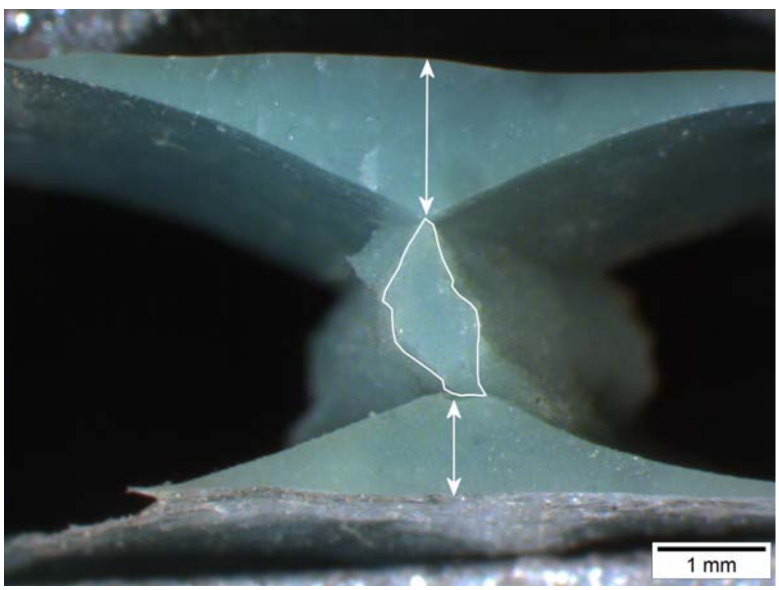


A cross section of a casting from an 8mm thick CTOA test specimen of X65 pipeline steel. The cross section is about 10 mm back from the tip of the crack and shows the shape of the "void" at this position. Extensive thinning through the thickness of the specimen is also apparent, because the outside surface of the casting approximates the original, un-thinned surface of the specimen.

In addition to supporting this effort through laboratory research, NIST representatives also attended the PHMSA R&D Forum in New Orleans in February and the Banff Workshop held in April.

**Reporting**

This is the third quarterly report under agreement number DTPH56-06-X-000029. The next quarterly report will be submitted in 3 months.